

Structural and Magnetic Properties of the Brownmillerite $\text{Ca}_2\text{Al}_x\text{Fe}_{2-x}\text{O}_5$ System

Gwe Ya Kim, Kwon Sun Roh, and Chul Hyun Yo

Department of Chemistry, Yonsei University, Seoul 120-749, Korea

Received June 21, 1995

A series of solid solutions in the $\text{Ca}_2\text{Al}_x\text{Fe}_{2-x}\text{O}_5$ ($x=0.00, 0.50, 0.66, 1.00$ and 1.34) system with brownmillerite structure has been synthesized at 1100°C under an atmospheric air pressure. The solid solutions are analysed by powder x-ray diffraction analysis, Mohr salt titration, thermal analysis, and Mössbauer spectroscopic analysis. The x-ray diffraction analysis assigns the compositions of $x=0.00$ and 0.50 to the space group $Pcmm$ and those of $x=0.66, 1.00,$ and 1.34 to the $Ibm2$. Mössbauer spectra have shown the coordination state and disordering of Al^{3+} and Fe^{3+} ions. The substituting preference of Al^{3+} ions for the tetrahedral site decreases with increasing x value. Magnetic susceptibility of the system has been measured in the temperature range of 5 K to 900 K . The solid solutions of the compositions of $x=0.00, 0.50$ and 0.66 have shown a thermal hysteresis and the thermoremanent magnetization gap decreases with increasing x value in the above systems. However the compositions of $x=1.00$ and 1.34 do not show the hysteresis. The exchange integral is calculated from Fe^{3+} ion occupancy ratio. The integral decreases with x value and thus the magnetic transition temperature decreases with the increasing x value.

Introduction

The crystal structure of the $\text{Ca}_2\text{Fe}_2\text{O}_5$ was first suggested by Büssel.¹ $Pcmm$ was considered to be the most probable space group with the basic structure consisted of layers of corner-sharing (AlO_6) octahedra alternating with layers of (FeO_4) tetrahedra. However Battle *et al.*² report that the atomic arrangement is similar to that proposed by Büssel but there is marked distortion of the oxygen octahedra and tetrahedra around the iron ions.

There was a considerable interest in the reorientation of the Fe^{3+} ion spins for magnetic properties of the $\text{Ca}_2\text{Fe}_2\text{O}_5$ system, which is similar to that of the orthoferrites. However the spin reorientation of the ion in the ErFeO_3 system is a continuous and coherent rotation of the Fe^{3+} ion spins.

In $Pcmm$, the c -direction is the direction only within the ac plane along which the spins can align without producing a ferromagnetic moment. The direction is probably preferred because of the large inter- and intra-superexchange bond angles. Battle *et al.*³ have observed thermal hysteresis in $\text{Ca}_2\text{Fe}_2\text{O}_5$ on cooling the material in a magnetic field from above the Néel temperature. They interpret the fact as the existence of a weak ferromagnetic moment parallel to a -axis.

Mössbauer spectroscopic study of the $\text{Ca}_2\text{Al}_x\text{Fe}_{2-x}\text{O}_5$ ($x \leq 1.0$) system shows the first order phase transition.⁴ The structure of the solid solutions with the high x value differs from that of $\text{Ca}_2\text{Fe}_2\text{O}_5$ and the most probable space group of the $\text{Ca}_2\text{AlFeO}_5$ is $Ibm2$.⁵

The site occupancy of Fe^{3+} and Al^{3+} ions in the brownmillerite structure has been of interest since Büssel hypothesized that all Fe^{3+} ions are in the tetrahedral sites and all Al^{3+} ions are in the octahedral sites. However Smith⁶ studied the intensities of the $0k0$ reflections versus composition. He predicted that the Al^{3+} ion substitutes preferentially in the tetrahedral sites until the tetrahedral sites are filled about half. Additional Al^{3+} ions are distributed equally into sites until $3/4$ and $1/4$ of the Al^{3+} ions in $\text{Ca}_2\text{AlFeO}_5$ system are located in tetrahedral and octahedral sites, respectively.

The Mössbauer spectroscopy indicates that the Al^{3+} ions are not restricted to the tetrahedral sites below $x=0.50$ and the cation distribution for $\text{Ca}_2\text{Al}_{0.5}\text{Fe}_{1.5}\text{O}_5$ is found to be $\text{Ca}_2[\text{Al}_{0.10}\text{Fe}_{0.90}](\text{Al}_{0.40}\text{Fe}_{0.60})\text{O}_5$ (in this paper [] and () represent octahedral and tetrahedral sites, respectively). Geller *et al.*⁴ investigated only hysteresis of $\text{Ca}_2\text{Fe}_2\text{O}_5$ but we expect thermal magnetic hysteresis with the change of x value.

In the present study, solid solutions of the $\text{Ca}_2\text{Al}_x\text{Fe}_{2-x}\text{O}_5$ system with compositions of $x=0.00, 0.50, 0.66, 1.00,$ and 1.34 have been prepared and their crystallographic structures and the valence state of iron ion are analyzed by powder x-ray diffraction analysis and Mohr salt titration, respectively. The magnetic properties of the system are discussed with the change of space group, Mössbauer spectroscopic analysis, and the magnetic measurement.

Experimental

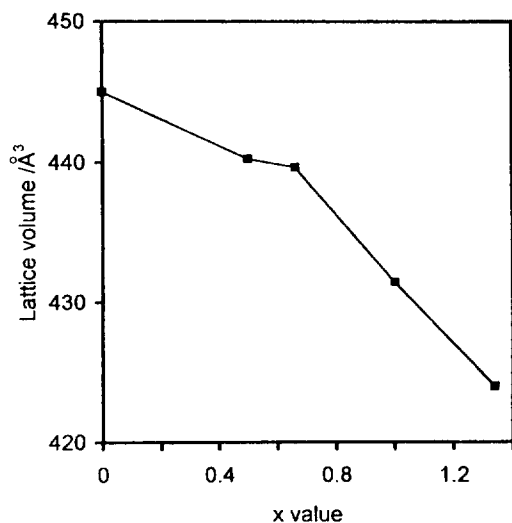
Samples of the $\text{Ca}_2\text{Al}_x\text{Fe}_{2-x}\text{O}_5$ system with compositions of $x=0.00, 0.50, 0.66, 1.00,$ and 1.34 have been prepared from the corresponding stoichiometric amounts of CaCO_3 (Sigma Chemical Co., 99.9%), Fe_2O_3 (Rare Metallic Co., 99.9%), and Al_2O_3 (Rare Metallic Co., 99.99%). The mixtures are heated at 800°C for 4 hrs to decompose the carbonate and after being ground, fired at 1100°C in the air for 48 hrs. The grinding and heating processes are repeated in order to produce a homogeneous solid solution.

The powder x-ray diffraction analysis has been carried out by a SIEMENS KRISTALLFLEX 805 using $\text{CuK}\alpha$ ($\lambda=1.5405\text{ \AA}$) radiation. The diffraction data are obtained by a fitting process with the Rietveld technique. The lattice parameters, the lattice volume of the unit cell, and the space group of the samples are also determined.

Thermal analysis has been carried out to examine the stability of the sample in the temperature range of 300 K - 1000 K and the analysis does not show any peak. The oxidation state of iron ions is specified as only Fe^{3+} state by Mohr salt titration.

Table 1. Lattice parameters, lattice volume, and space group of solid solutions for the $\text{Ca}_2\text{Al}_x\text{Fe}_{2-x}\text{O}_5$ system

x value	Lattice parameter/Å			Lattice volume/Å ³	Space group
	a	b	c		
0.00	5.58(6)	14.74(7)	5.41(4)	446.0(1)	<i>Pcmm</i>
0.50	5.58(8)	14.63(2)	5.38(4)	440.2(2)	<i>Pcmm</i>
0.66	5.58(5)	14.61(7)	5.38(5)	439.6(1)	<i>Ibm2</i>
1.00	5.55(2)	14.50(6)	5.35(7)	431.4(8)	<i>Ibm2</i>
1.34	5.52(1)	14.46(1)	5.31(1)	424.0(2)	<i>Ibm2</i>

**Figure 1.** Plot of lattice volume versus x value for solid solutions of the $\text{Ca}_2\text{Al}_x\text{Fe}_{2-x}\text{O}_5$ system.

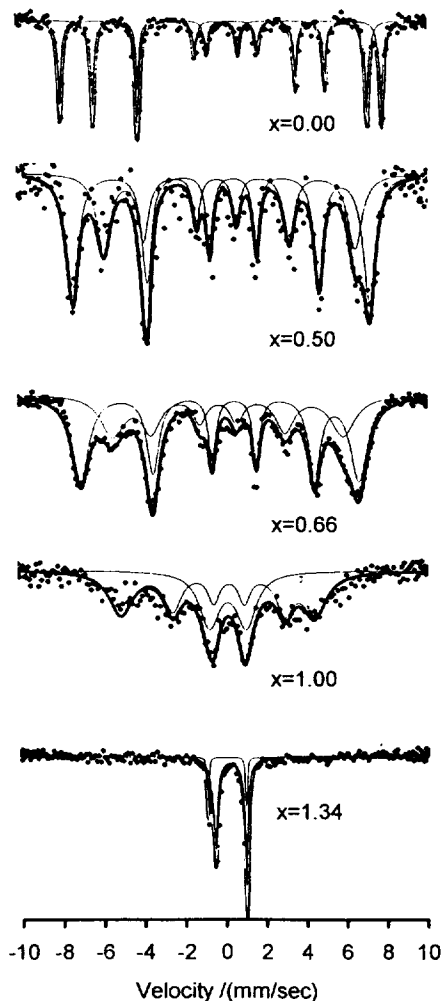
The Mössbauer spectroscopic analysis has been performed in the standard transmission geometry using a source of ^{57}Co in Rh matrix. The spectra are recorded at room temperature and fitted using a least-squares refinement program.

Magnetic measurement has also carried out by a Faraday Balance Magnetometer and a SQUID in the temperature range from 5 K to 900 K. The heating and cooling processes are followed in order to show the thermal magnetic hysteresis.

Results and Discussion

The x-ray diffraction patterns of solid solutions with compositions corresponding to $x=0.00, 0.50, 0.66, 1.00,$ and 1.34 are indexed on the basis of the orthorhombic unit cell of the brownmillerite structure. The intensities of $h0l$ peaks with the conditions of $h+l=2n+1$ decrease with increasing x value and are near zero at the composition of $x=0.66$. Therefore the compositions of the $0.00 \leq x < 0.66$ correspond to the space group *Pcmm* (D_{2h}^{16}) and those of the $0.66 \leq x < 1.34$ to the *Ibm2* (C_{2v}^{22}).⁵ The accurate lattice parameters of the $\text{Ca}_2\text{Al}_x\text{Fe}_{2-x}\text{O}_5$ compounds have been calculated from the above space groups by a Rietveld technique based on the analytical least-squares refinement. The lattice parameters, lattice volume, and space group are listed in Table 1.

The lattice volume decreases with increasing x value with

**Figure 2.** Mössbauer spectra of the $\text{Ca}_2\text{Al}_x\text{Fe}_{2-x}\text{O}_5$ system at room temperature.

anomaly at the $x=0.66$ where phase transition⁴ occurs as shown in Figure 1. The decreasing lattice volume is due to the substitution of the smaller Al^{3+} ion (50 pm) for the larger Fe^{3+} ion (64 pm).

The experimental data of DTA and TGA for all the compositions show that there is neither weight loss nor phase transition in the temperature range of 300 K-1000 K. The compounds, therefore, might be thermally stable in the condition. It means that the orthorhombic phase and oxidation state of Fe^{3+} ion, assuming the stable electronic structure of Ca^{2+} and Al^{3+} ions, are retained in the above temperature range.⁷

The Mössbauer spectra of the $\text{Ca}_2\text{Al}_x\text{Fe}_{2-x}\text{O}_5$ system are shown in Figure 2. The spectra are fitted with Lorentzian curves and the Mössbauer parameters are listed in Table 2. They show that the solid solutions of all the compositions contain only the oxidation state of Fe^{3+} ion and have the brownmillerite orthorhombic structure in which the layers of $[\text{FeO}_6]$ octahedra and of (FeO_4) tetrahedra are alternating along b-axis.

The compositions of $x=0.00, 0.50,$ and 0.66 show spectra of the magnetic materials below the magnetic ordering temperature. The ordering of magnetic spins of Fe^{3+} ions can be explained by superexchange model.⁸ The exchange inter-

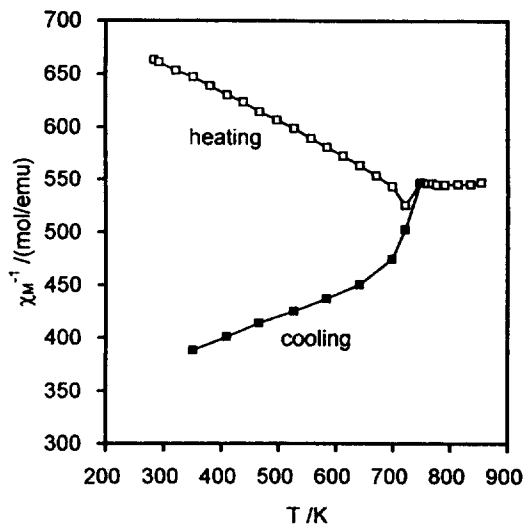
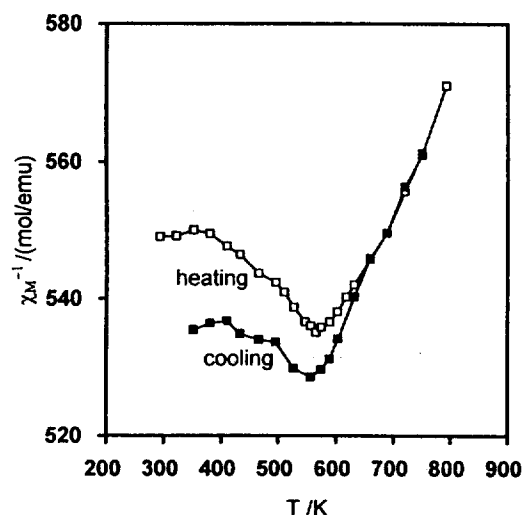
Table 2. Mössbauer parameters such as isomer shift (δ), quadrupole splitting (ΔE_q), hyperfine field (H_{int}), linewidth (Γ), and Al (tet)/Al(oct) for solid solutions of the $\text{Ca}_2\text{Al}_x\text{Fe}_{2-x}\text{O}_5$ system

x value	Fe site	δ /(mm/sec)	ΔE_q /(mm/sec)	H_{int}/Γ	Γ /(mm/sec)	Al(T)/ Al(O)
0.00	Fe(O)	0.37(9)	-0.53(6)	50.1(3)	0.25	-
	Fe(T)	0.21(3)	0.70(4)	42.7(4)	0.25	
0.50	Fe(O)	0.37(2)	-0.59(2)	46.2(4)	0.73	3.17
	Fe(T)	0.17(3)	0.66(7)	39.1(7)	0.86	
0.66	Fe(O)	0.35(0)	-0.70(7)	43.5(1)	1.03	2.14
	Fe(T)	0.15(9)	0.50(8)	36.0(1)	1.00	
1.00	Fe(O)	0.34(9)	1.86(2)	-	1.21	-
	Fe(T)	0.13(5)	-0.54(7)	30.2(5)	1.39	
1.34	Fe(O)	0.23(5)	1.52(7)	-	0.28	1.83
	Fe(T)	0.05(9)	1.89(5)	-	0.26	

action between the Fe^{3+} ions occurs *via* an induced spin density in the s orbital of diamagnetic Al^{3+} ion by a polarized p orbital on the oxygen ion due to paramagnetic Fe^{3+} ion. The spectrum for the composition of $x=0.00$ can be fitted by using two series of sextets with the same intensity as shown in Figure 2. The isomer shift of 0.37(9) mm/sec and hyperfine field of 50.1(3) T for the first sextet are consistent with the Fe^{3+} ion at the octahedral site. Those of 0.21(3) mm/sec and 42.7(4) T for the second sextet allow us to attribute to the Fe^{3+} ion at the tetrahedral site.^{9,10}

For compositions of $x=0.50$ and 0.66, the isomer shift of the sextet with high intensity and that of another sextet with low intensity correspond to the Fe^{3+} ion at the octahedral site and that at the tetrahedral site, respectively. Mössbauer spectrum for the composition of $x=1.00$ can be fitted by assuming a doublet with isomer shifts of 0.34(9) mm/sec and a sextet of 0.13(5) mm/sec. The doublet and sextet are consistent with Fe^{3+} ions at octahedral and tetrahedral sites, respectively. It seems that the transition temperature of magnetic ordering may be near the room temperature for the composition of $x=1.00$. Mössbauer spectrum of the $x=1.34$ is one of the paramagnetic compound and corresponds to the Fe^{3+} ions at octahedral and tetrahedral sites.

The isomer shift decreases with increasing x value and thus the covalency between Fe^{3+} and O^{2-} ions increases with x value, which reflects the decreasing lattice volume and the increasing ionic character of $\text{Al}^{3+}\text{-O}^{2-}$ bond. The very low isomer shift of the composition of $x=1.34$ supports that $[\text{FeO}_6]$ octahedron and (FeO_4) tetrahedron are majorly surrounded by the Al^{3+} ion with more ionic character, which will be discussed latter on. The linewidths of the compositions of $x=0.50$, 0.66, and 1.00 are large and are reasonable for disordering of Al^{3+} and Fe^{3+} ions in each octahedral and tetrahedral layer, respectively. In the disordering system of Al^{3+} and Fe^{3+} ions the possible atomic arrangements such as $(\text{FeO}_x)\text{Fe}_x$, $(\text{FeO}_x)\text{Fe}_{x-1}\text{Al}$, $(\text{FeO}_x)\text{Fe}_{x-2}\text{Al}_2$, $(\text{FeO}_x)\text{Fe}_{x-3}\text{Al}_3$, etc, where x is 4 and 6, allow central Fe^{3+} ions to have slightly different Mössbauer parameters, which induces the broadening of Mössbauer lines.¹¹ The sharp linewidth of the $x=1.34$ means that $[\text{FeO}_6]$ octahedron and (FeO_4) tetrahedron are majorly not surrounded by Fe^{3+} ions but by Al^{3+}

**Figure 3.** Plot of χ_M^{-1} versus T for the $\text{Ca}_2\text{Fe}_2\text{O}_5$ system.**Figure 4.** Plot of χ_M^{-1} versus T for the $\text{Ca}_2\text{Al}_{0.5}\text{Fe}_{1.5}\text{O}_5$ system.

ions, which is consistent with lower Néel temperature as shown in Figure 6.

The ratio Al(T)/Al(O) in each composition has been calculated from the ratio between peak areas of Fe^{3+} ions at octahedral and tetrahedral sites as listed in Table 2.¹² Thus the cation distributions for the $\text{Ca}_2\text{Fe}_{2-x}\text{Al}_x\text{O}_5$ system are found to be $\text{Ca}_2\text{Fe}\text{O}_5$ for the $x=0.00$, $\text{Ca}_2[\text{Al}_{0.12}\text{Fe}_{0.88}](\text{Al}_{0.38}\text{Fe}_{0.62})\text{O}_5$ for the $x=0.50$, $\text{Ca}_2[\text{Al}_{0.21}\text{Fe}_{0.79}](\text{Al}_{0.45}\text{Fe}_{0.55})\text{O}_5$ for the $x=0.66$, and $\text{Ca}_2[\text{Al}_{0.47}\text{Fe}_{0.53}](\text{Al}_{0.97}\text{Fe}_{0.14})\text{O}_5$ for the $x=1.34$. Although the Al^{3+} ion with the small ionic radius (50 pm) prefers the tetrahedral site, the ratio of Al^{3+} ion between the both sites decreases with x value, which agrees with Smith's work⁶ in the introduction.

Plots of reciprocal molar magnetic susceptibilities versus temperature are shown in Figures 3-6. Magnetic parameters such as Néel temperature, Curie constant (C), paramagnetic Curie temperature (θ_p), and effective magnetic moment (μ_{eff}) obtained from the plots are listed in Table 3. The magnetic behavior of the $\text{Ca}_2\text{Al}_x\text{Fe}_{2-x}\text{O}_5$ below the Néel temperature

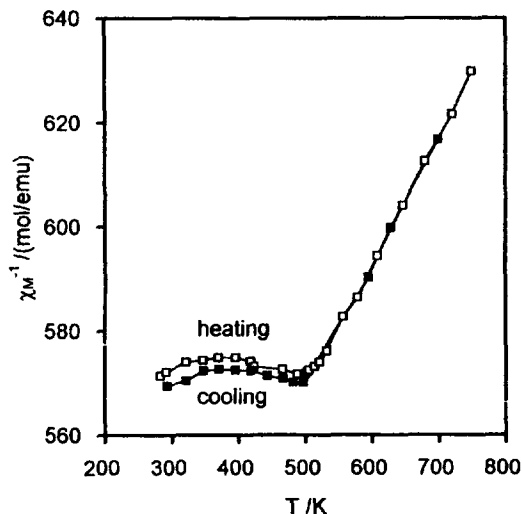


Figure 5. Plot of χ_M^{-1} versus T for the $\text{Ca}_2\text{Al}_{0.66}\text{Fe}_{1.34}\text{O}_5$ system.

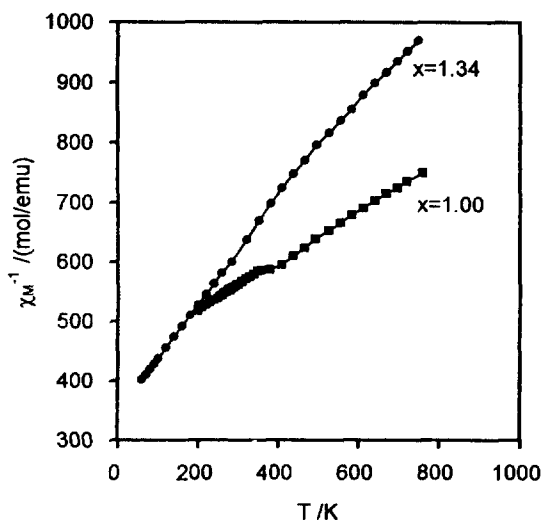


Figure 6. Plots of χ_M^{-1} versus T for the compositions of $x=1.00$ and 1.34 of the $\text{Ca}_2\text{Al}_x\text{Fe}_{2-x}\text{O}_5$ system.

can be described by the superexchange model in which the antiparallel arrangement of magnetic spins of Fe^{3+} ions is predominant as shown by the negative paramagnetic Curie temperature. The substitution of a diamagnetic Al^{3+} ion for Fe^{3+} ion reduces the Néel temperature as listed in Table 3, which is consistent with the decreasing hyperfine field at Fe^{3+} ion as listed in Table 2. The effective magnetic moment of the $\text{Ca}_2\text{Al}_x\text{Fe}_{2-x}\text{O}_5$ system is slightly smaller than that of spin-only magnetic moment of high spin Fe^{3+} ions, which means that the short range spin ordering is present in a paramagnetic region.

The compositions of $x=0.00-0.66$ show thermal hysteresis on cooling the material in a magnetic field of 6300 kOe below the Néel temperature. The hysteresis does not take place by the crystal phase change because the crystal phases of the solid solutions are not changed during the heating and cooling. The frustration produced by substitution of diamagnetic Al^{3+} ion in place of Fe^{3+} ion in the compositions of $x=0.50$ and 0.66 is unreasonable because of a large concen-

Table 3. Magnetic parameters and the effective magnetic moment (μ_{eff}) for solid solutions of the $\text{Ca}_2\text{Al}_x\text{Fe}_{2-x}\text{O}_5$ system

x value	T_N/K	C	Θ_p	$\mu_{\text{eff}}/\text{B.M}$
0.00	721	—	—	—
0.50	575	5.57	-462	6.67
0.66	499	4.04	-444	5.68
1.00	350	2.31	-423	4.30
1.34	—	1.25	-358	3.16

Table 4. Exchange integral between Fe^{3+} ions for the $\text{Ca}_2\text{Al}_x\text{Fe}_{2-x}\text{O}_5$ system

x value	z	$-J/k/\text{K}$
0.00	5.00	24.72
0.50	4.03	24.46
0.66	3.61	23.70
1.34	2.17	below 0.40

tration of paramagnetic Fe^{3+} ions.¹³ The thermal hysteresis is the same as that observed in many orthoferrites where the spin reorientation of Fe^{3+} ion is induced by the anisotropy due to the spin ordering of rare earth metal ion.

The hysteresis in the compositions of $x=0.00$ and 0.50 with the space group of $Pcmn$ is due to the correlation between the spin direction and the local anisotropic field which can be interpreted in terms of the Dzyaloshinsky-Moriya interaction.¹³ In $Pcmn$ the c -direction is the only direction which the spins can align without producing a ferromagnetic moment. However hysteresis gap and preference of c -direction are decreased with decreasing of paramagnetic Fe^{3+} ion. The hysteresis gap disappears at the compositions of $x=1.00$ and 1.34 with space group of $Ibm2$ which results in more restriction on the spin direction.⁴ Although the space group of the composition of $x=0.66$ is $Ibm2$, the small hysteresis gap means that the composition contains a small amount of phase with space group of $Pcmn$. The composition of $x=1.00$ shows a weak ferromagnetism due to the spin canting induced by a distortion of the sublattice, which is consistent with large quadrupole splitting as shown in Table 2.^{14,15} The composition of $x=1.34$ does not show any slope change of the plot of χ_M^{-1} versus T in the range of 5 K to 760 K.

In the molecular field theory, the exchange integral, $|J|/k$, for an antiferromagnet can be estimated from the following relation.

$$|J|/k = \frac{-3 \times T_N}{z \times S(S+1)}$$

where k is Boltzman constant, S the spin, equal to $5/2$ for the high spin Fe^{3+} ion, and z the number of nearest neighbor Fe^{3+} ions. The number of nearest neighbor Fe^{3+} ions for a Fe^{3+} ion is the statistical summation of $4[\text{Fe}^{3+}] + 2(\text{Fe}^{3+})$ and $2[\text{Fe}^{3+}] + 2(\text{Fe}^{3+})$ in the octahedral and tetrahedral sites, respectively. As listed in Table 4, the exchange integral decreases with the increasing x value in the compositions of $x=0.00-0.66$ and shows anomalous small value at the composition of $x=1.34$. The small intergral is consistent with

the abruptly decreased isomer shift and narrow linewidth of the Mössbauer spectrum and the low Néel temperature at the composition of $x=1.34$.

Conclusion

Solid solutions of all the compositions have brownmillerite structure. The Al^{3+} ion with the smaller ionic radius prefers the tetrahedral site but the preference decreases at the increased x value. The Al^{3+} and Fe^{3+} ions are randomly distributed in each octahedral and tetrahedral sites. The substitution of diamagnetic Al^{3+} ion in place of paramagnetic Fe^{3+} ion decreases the exchange integral. The Fe^{3+} ion is isolated by diamagnetic ions at the composition of $x=1.34$ and the composition has no long range ordering of Fe^{3+} ion spins above 5 K. The composition of $x=1.34$ may be below the percolation threshold of a Heisenberg antiferromagnet. The Fe^{3+} ion is high spin state and thus isotropic. The spin direction can be changed by local anisotropic field in the compositions of $x=0.00-0.66$ with space group of *Pcmn*. However the compositions of $x=1.00$ and 1.34 do not show spin re-orientation when cooling due to high symmetric space group of *Ibm2*.

Acknowledgment. This work was supported by grant No. 92-25-00-02 from the Korea Science and Engineering Foundation in 1993 and therefore we express our appreciation to the authorities concerned.

References

1. Büssem, *Fortschr. Min.* 1937, 22, 31.
2. Colville, A. A. *Acta Cryst.* 1970, B26, 1469.
3. Battle, P. D.; Bollen, S. K.; Gibb, T. C.; Matsuo, M. *J. Solid State Chem.* 1990, 90, 42.
4. Geller, S.; Grant, R. W.; Fullmer, I. D. *J. Phys. Chem. Solids* 1970, 31, 793.
5. Battle, P. D.; Gibb, T. C.; Lightfoot, P. J. *Solid State Chem.* 1988, 76, 334.
6. Smith, D. K. *Acta Cryst.* 1962, 15, 1146.
7. Shin, S.; Yonemura, M.; Ikawa, H. *Bull. Chem. Soc. Japan* 1979, 52, 947.
8. Gibb, T. C. *J. Chem. Soc., Dalton Trans.* 1983, 873.
9. Grenier, J. C.; Fournés, L. *Mat. Res. Bull.* 1982, 17, 55.
10. Gibb, T. C. *J. Solid State Chem.* 1990, 88, 485.
11. Gibb, T. C. *J. Chem. Soc., Dalton Trans.* 1983, 2031.
12. Grenier, J. C.; Pouchard, M. *J. Solid State Chem.* 1975, 13, 92.
13. Rodriguez, R.; Frenández, A.; Isalgué, A.; Rodriguez, J.; Labarta, A.; Teiada, J.; Obradors, X. *J. Phys. C: Solid State Phys.* 1985, 18, L 401.
14. Yo, C. H.; Lee, E. S.; Pyon, M. S. *J. Solid State Chem.* 1988, 73, 411.
15. Yo, C. H.; Kim, H. R.; Ryu, K. H.; Roh, K. S.; Choy, J. H. *Bull. Kor. Chem. Soc.* 1994, 15, 636.

Hydrolysis of *p*-Nitrophenyl Acetate and *p*-Nitrophenyldiphenyl Phosphate in Micellar Solution by *N*-Chloro Compounds: Involvement of Counter Ions in Micellar Catalysis

Byeong-Deog Park[†] and Yoon-Sik Lee*

Department of Chemical Technology, Seoul National University, Seoul 151-742, Korea

[†]Aekyung Ind. Co., LTD., Central Research Lab., Taejon 300-200, Korea

Received June 24, 1995

Hydrolysis of *p*-nitrophenyl acetate (PNPA) and *p*-nitrophenyldiphenyl phosphate (PNPDPP) by *N*-chloro compounds in micellar solution were studied. *N,N'*-Dichloroisocyanuric acid sodium salt (DCI) in cetyltrimethylammonium chloride (CTACl) micellar solution gave pseudo first-order kinetics. But, DCI in cetyltrimethylammonium bromide (CTABr) micellar solution showed typical series first-order kinetics - fast hydrolysis of the esters and concomitant slow decay of the hydrolyzed product, *p*-nitrophenolate. The hydrolysis rate was decreased as the hydrophobicity of *N*-chloro compounds was increased, which is the opposite trend to the usual bimolecular micellar reaction. This curious behavior of the *N*-chloro compounds in the catalytic hydrolysis of PNPA and PNPDPP in a cationic micellar system can be best explained by participation of counter ions of the surfactants during hydrolysis.

Introduction

As a mimic system of enzyme catalysis and a model system for destruction of nerve agents, the hydrolysis of *p*-nitrophenyl acetate (PNPA) and *p*-nitrophenyldiphenyl phosphate (PNPDPP) in either micellar or microemulsion system has been extensively investigated.¹ We had previously repor-

ted some interesting results of the hydrolysis of PNPA by *N,N'*-dichloroisocyanuric acid sodium salts (DCI) in cationic micellar system.² In that paper, we concluded that the difference in the reactivity of the catalytic hydrolysis of PNPA by DCI in various cationic micellar systems were due to formation of different halogen species which were formed by the reaction between the counter ions of the surfactant